This is an open access article published under an ACS AuthorChoice License, which permits copying and redistribution of the article or any adaptations for non-commercial purposes.

JACS
JOURNAL OF THE AMERICAN CHEMICAL SOCIETY
Article
pubs.acs.org/JACS

Substantial Expansion of Detectable Size Range in Ionic Current Sensing through Pores by Using a Microfluidic Bridge Circuit

Hirotoshi Yasaki,[*,†,‡] Takao Yasui,[*,†,‡,§] Takeshi Yanagida,[*,∥,⊥] Noritada Kaji,[†,‡,§] Masaki Kanai,[∥] Kazuki Nagashima,[∥] Tomoji Kawai,[*,⊥] and Yoshinobu Baba[*,†,‡,#]

[†]Department of Biomolecular Engineering, Graduate School of Engineering, Nagoya University, Furo-cho, Chikusa-ku, Nagoya 464-8603, Japan

[‡]ImPACT Research Center for Advanced Nanobiodevices, Nagoya University, Furo-cho, Chikusa-ku, Nagoya 464-8603, Japan

[§]Japan Science and Technology Agency (JST), PRESTO, 4-1-8 Honcho, Kawaguchi, Saitama 332-0012, Japan

[∥]Laboratory of Integrated Nanostructure Materials Institute of Materials Chemistry and Engineering, Kyushu University, 6-1 Kasuga-koen, Kasuga, Fukuoka 816-8580, Japan

[⊥]Institute of Scientific and Industrial Research, Osaka University, Mihogaoka, Ibaraki, Osaka 567-0047, Japan

[#]Health Research Institute, National Institute of Advanced Industrial Science and Technology (AIST), Takamatsu, Kagawa 761-0395, Japan

Supporting Information

ABSTRACT: Measuring ionic currents passing through nano- or micropores has shown great promise for the electrical discrimination of various biomolecules, cells, bacteria, and viruses. However, conventional measurements have shown there is an inherent limitation to the detectable particle volume (1% of the pore volume), which critically hinders applications to real mixtures of biomolecule samples with a wide size range of suspended particles. Here we propose a rational methodology that can detect samples with the detectable particle volume of 0.01% of the pore volume by measuring a transient current generated from the potential differences in a microfluidic bridge circuit. Our method substantially suppresses the background ionic current from the μA level to the pA level, which essentially lowers the detectable particle volume limit even for relatively large pore structures. Indeed, utilizing a microscale long pore structure (volume of 5.6×10^4 aL; height and width of 2.0×2.0 μm; length of 14 μm), we successfully detected various samples including polystyrene nanoparticles (volume: 4 aL), bacteria, cancer cells, and DNA molecules. Our method will expand the applicability of ionic current sensing systems for various mixed biomolecule samples with a wide size range, which have been difficult to measure by previously existing pore technologies.

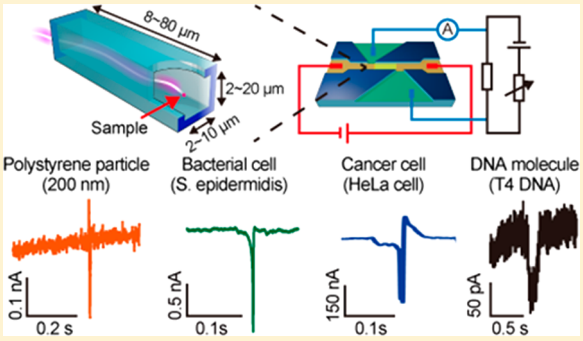

INTRODUCTION

Ionic current sensing methods using nano- or micropores can provide electrical signals with information on size and concentration for viruses,[1−3] bacteria,[4] and human cells,[5] and various biomolecules including DNA,[6−12] RNA,[13,14] and protein molecules.[15−21] The detection mechanism is based on the electrical resistance increase of the pore in response to the excluded volume due to the introduced objects when applying electrical voltages. Previously, studies have probed the ability of these ionic current sensing methods for size detection (error, less than 1%) and high throughput detection (>10^2 counts per minute).[22,23] However, the existing approaches have an inherent limitation for the detectable particle volume (1% of pore volume),[2,4,5,14,24−27] which critically restricts applications of these methods for mixture samples with a wide size range of suspended particles (Figures 1a and S1). Because the size distributions of real biomolecule samples tend to be wide, this limitation of ionic current sensing is critical for real applications. Additionally, although the major efforts in ionic current sensing have been directed toward using smaller pores for higher resolution,[28] clogging of small pores by the samples is a critical issue in applying the ionic current sensing methods to real biomolecule samples. The particle volume resolution of existing ionic current sensing methods is limited by the background ionic current.[5,6,16] Because a small object in a large pore (with respect to width or length) exhibits a small signal, it tends to be difficult to discriminate the current signal of the small object from the current baseline noise. In addition, large ionic currents cause a high background ionic current exceeding the limit of current detection. Thus, it seems to be rather

Received: June 26, 2017
Published: September 7, 2017

© 2017 American Chemical Society

DOI: 10.1021/jacs.7b06440
J. Am. Chem. Soc. 2017, 139, 14137−14142

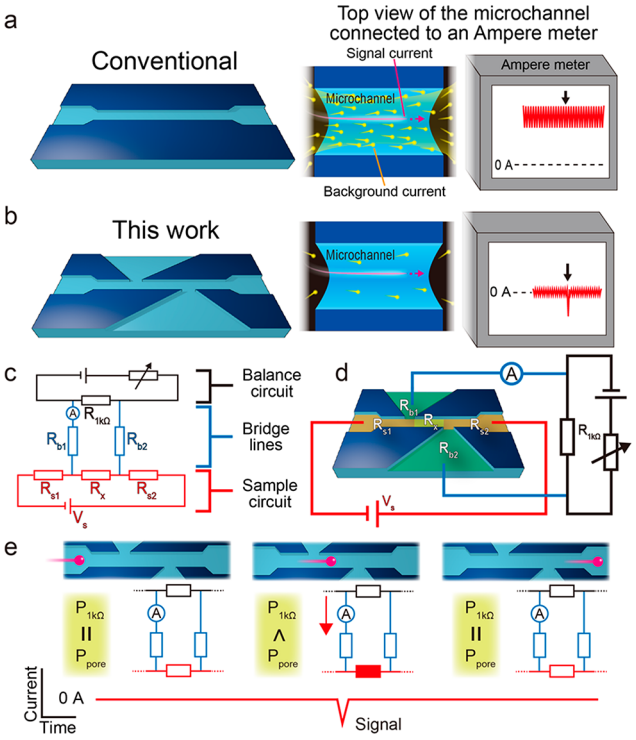

Figure 1. Conceptual illustrations for the microfluidic bridge circuit. (a) Schematic illustration for particle detection using the conventionally reported methods. (b) Schematic illustration for particle detection using our proposed method. (c) Diagram of our proposed bridge circuit: red lines are for the sample circuit, blue lines are for bridge lines, and black lines are for the balance circuit. The sample circuit has a voltage source (V_s) and resistors for the micropore (R_x) and sample flow channels (R_{s1} and R_{s2}). The bridge lines have resistances for them (R_{b1} and R_{b2}) and an Ampere meter (A), and the balance circuit has a 1-kΩ resistor ($R_{1\text{-k}\Omega}$). (d) Our proposed microfluidic bridge circuit; the micropore is the yellow area (R_x), sample flow channels are marked as orange areas (R_{s1} and R_{s2}), and bridge channels are marked as green areas (R_{b1} and R_{b2}). (e) Schematic illustrations, electric circuit diagrams, and schematic current value in the microfluidic bridge circuit. The red filled rectangle shows increased resistance by sample introduction. The red arrow shows flow direction of current by deviation of potential differences between the two circuits, sample and balance. $P_{1\text{-k}\Omega}$ and P_{pore} show potential differences of both ends for the 1-kΩ resistor and the micropore, respectively.

difficult for relatively large pores, which can avoid pore clogging by samples, to detect a small sample using existing approaches.

Here, we propose a rational methodology using a microfluidic bridge circuit, which suppresses the background ionic current from the μA level to the pA level, even under high applied voltages, for small object detection in large pores (Figure 1b). The microfluidic bridge circuit essentially drops the lower limit of the detectable particle volume range even for relatively large pore structures, as shown in Figure S1. Because our method does not rely on the flowing ionic current that includes the background ionic current, it overcomes the inherent imitation of the conventional methods. The detectable particle volume can be lowered to 0.01% of the pore volume.

RESULTS AND DISCUSSION

Our proposed methodology using a microfluidic bridge circuit enabled us to detect small current signals, which are undetectable in conventional methods, by suppressing the background current (Figure 1a,b). The methodology has great promise for analyzing nanoparticles, bacterial cells, human cancer cells, and DNA molecules as discussed later. Figure 1c shows the circuit diagram implementing our method, which connects a circuit for balancing potential (balance circuit) to a circuit for sample flow (sample circuit) via bridge lines that include an Ampere meter. This design isolates the Ampere meter for ionic current measurements from the sample circuit, although the Ampere meter is conventionally set in the sample circuit. The second point of our method is to use a balancing potential in a microfluidic bridge circuit. Under the balanced potential state in a microfluidic bridge circuit, ionic currents can be minimized by controlling the variable resistance. Because microfluidic channels act as a resistor, we can depict a circuit diagram of the microfluidic bridge circuit consisting of a micropore (yellow area), sample flow channels (orange areas), and bridge channels (green areas) with the off-channel 1-kΩ resistor and a variable resistor, Ampere meter, and voltage source, as shown in Figure 1d. When a sample enters the micropore, the balanced potential is transiently collapsed, which generates a transient current (Figure 1e). The potential difference between both ends of the 1-kΩ resistor ($P_{1\text{-k}\Omega}$) is set equal to that of the micropore (P_{pore}) by the variable resistance before sample introduction (left images in Figure 1e), and then, when the sample enters the micropore, the resistance value of the micropore increases, and then P_{pore} also increases (P_{pore} becomes larger than $P_{1\text{-k}\Omega}$) (middle images in Figure 1e). Figure 2 shows the fabricated microfluidic bridge circuit devices

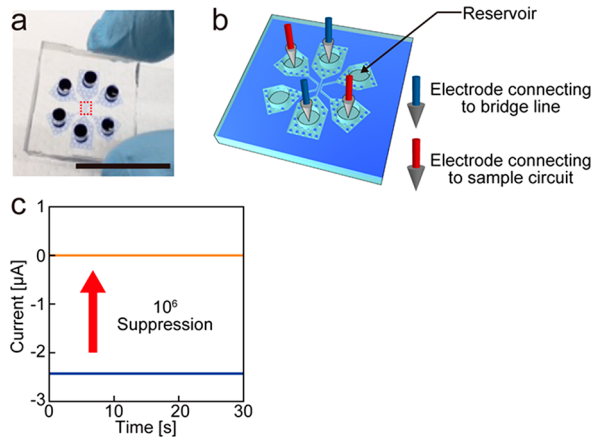

Figure 2. Background ionic current suppression using the microfluidic bridge circuit. (a) Photo of the fabricated PDMS chip; scale bar, 2 cm. (b) Schematic illustration for a microfluidic channel with electrodes. (c) Background ionic current suppression from the conventional circuit to the bridge circuit. Blue and orange lines show background ionic current in the conventional circuit (2.45 μA, blue line) and in the bridge circuit (6.28 pA, orange line) under the applied voltage of 53 V. The height, width, and length of the micropore were 7.5, 4.0, and 80 μm, respectively.

and some measured data. The microchannel of the poly(dimethylsiloxane) (PDMS) chip was filled with electrolyte solution. In this paper, we used 5×TBE buffer (0.45 M Tris, 0.45 M boric acid, 0.01 M EDTA) as the standard electrolyte solution. The electrodes for the sample circuit and the bridge lines into the reservoirs were inserted as shown in Figure 2b. When we measured the ionic current for the sample circuit, the background current was 2.45 μA under the applied voltage of 53 V. By using the balanced potential circuit, the background current was substantially suppressed to 6.28 pA, as shown in

DOI: 10.1021/jacs.7b06440
J. Am. Chem. Soc. 2017, 139, 14137−14142

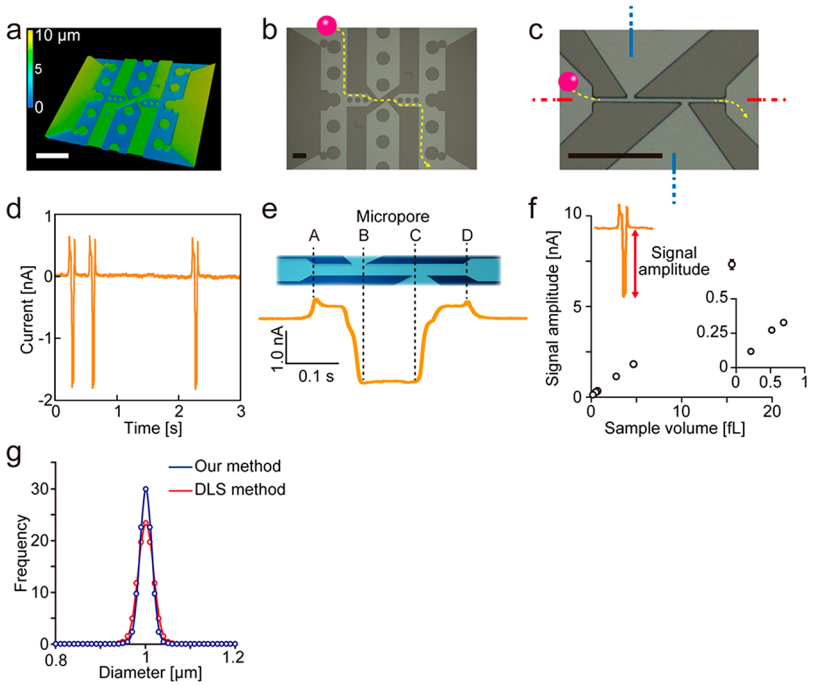

Figure 3. Particle detection using the microfluidic bridge circuit. (a) 3D image of the center in Figure 2a; scale bar, 300 μm. (b, c) Sample injection schemes; scale bars, 100 μm. Dimensions of micropore were 7.5 μm height × 4.0 μm width × 80 μm length. (d) Signals for 2.08 μm diameter particles. Applied voltage was 12 V. (e) Schematic illustration of the micropore and the signal for 2.08 μm diameter particles. The letters A, B, C, and D are positions around the micropore. (f) Signal amplitude of 0.75, 1.00, 1.10, 1.75, 2.08, and 3.10 μm diameter particles. Applied voltage was 53 V. Error bars show the standard deviation for a series of measurements (N = 200). (g) Comparison of the size distribution for 1.00 μm diameter particles obtained using our method and the DLS method.

Figure 2c. The background current suppression is accomplished by balancing potentials of the two circuits, sample and balance, by adjusting the variable resistor.

Figure 3a–c shows photographs of microfluidic devices employed for the ionic current sensing measurements of polystyrene particles and sample injection schemes. Figure 3d shows signals of ionic current in a microfluidic bridge circuit when electrophoretically introducing particles (diameter of 2.08 μm) into the micropore. We tried to detect particles in a conventional series circuit, having the same micropore structure, and using the same applied voltage; however, the current signals by particles were buried in the noise and could not be detected, because small current changes became unmeasurable at low detection gain of the amplifier, which is necessary for measuring large currents (the calculated signal amplitude in the series circuit was smaller than 10 nA, theoretically). Unique signal shapes were observed, as exemplified in Figure 3e. The measured current first increased and showed a peak. After the peak, the current decreased and showed a constant value for a while, and then increased to a second peak. Our microscope observation revealed that these signal shapes strictly corresponded to the spatial location of particles within the micropore (Figure 3e). When the first peak appeared, the particle was located at position A. When the current started to decrease and became constant, the particle was at positions between B and C. When the current increased and showed the second peak, the particle was at position D. These unique signatures in the measured ionic current signals can be interpreted in terms of a transient current of unbalanced potential in the microfluidic bridge circuit due to the entry of particles into the micropore. Thus, the measured ionic current of the microfluidic bridge circuit contains interesting spatial information about the particles within the micropore. The overlay of 100 signals showed the same shapes, and this proved the high reproducibility of our method (Figure S2). The tendency of a longer micropore to show a smaller signal amplitude and longer translocation time (Figure S3) was consistent with findings of the conventional ionic current sensing methods. To explore the applicability of the microfluidic bridge circuit for wide sample size range, we measured ionic current for polystyrene particles whose diameters ranged from 0.75 to 3.10 μm. Figure 3f shows the signal amplitude, which is defined as the difference between the current value at the baseline and the current value at the lowest point of the measured signals, when varying the particle size (i.e., volume). The linear relationship between the particle volume and the measured signal amplitude seen in the figure highlights the accuracy of the present microfluidic bridge circuit for the studied sample size range. Therefore, the present microfluidic bridge circuit can estimate the particle size distribution from the measured signal amplitude data. This ionic current sensing method in principle measures an "individual" particle to extract the size distribution, which is in sharp contrast to the conventional dynamic light scattering (DLS) method that is based on size measurements with the assumption of a Gaussian distribution. Figure 3g compares the measured size distribution of the present method and the reference data with the DLS method when measuring polystyrene particles (mean diameter of 1.00 μm). Measured data showed the size distribution was slightly narrower than the reference data, although the mean value and standard deviation were quite similar.

To further enhance the sensitivity of our present method, we examined the effects of several measurement parameters of the microfluidic bridge circuit including applied voltages, micropore

DOI: 10.1021/jacs.7b06440
J. Am. Chem. Soc. 2017, 139, 14137–14142

channel geometry, and electrolyte solution resistivity. Figure 4a shows the effect of applied voltage (range from 30 to 80 V) on

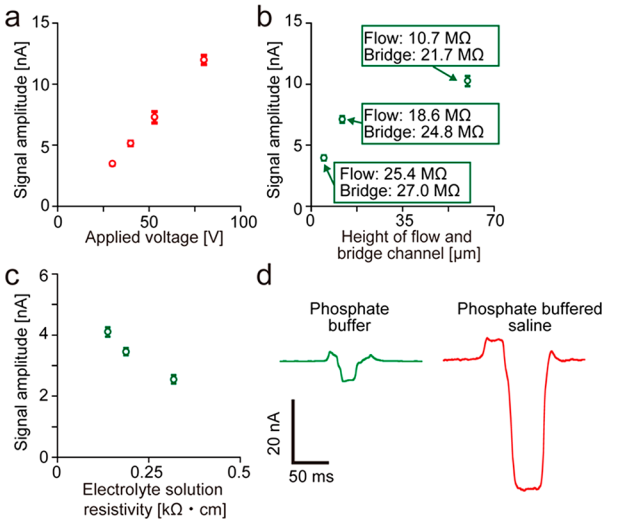

Figure 4. Effect of applied voltages, microchannel resistance, and buffer resistivity on signal amplitude. (a) Detection of 3.10 μm diameter particles under the applied voltages of 30, 40, 60, or 80 V; micropore dimensions of 7.5 μm height × 4.0 μm width × 80 μm length. (b) Detection of 1.00 μm diameter particles with different heights of the sample flow channels and bridge channels (5, 12, and 60 μm); micropore dimensions of 2.0 μm height × 2.0 μm width × 14 μm length. "Flow" and "Bridge" mean resistances of the sample flow channels and bridge channels, respectively. (c) Detection of 1.00 μm diameter particles with different concentrations of electrolyte solution (5×TBE buffer, 0.319 kΩ·cm; 10×TBE buffer, 0.188 kΩ·cm; 20×TBE buffer, 0.138 kΩ·cm); micropore dimensions of 6.6 μm height × 4.5 μm width × 16 μm length. Error bars in panels a, b, and c show the standard deviation for a series of measurements (N = 200). (d) Signals for detection of 3.10 μm diameter particles in phosphate buffer (0.376 kΩ·cm, 13 mM sodium hydrogen phosphate, 6.5 mM sodium dihydrogen phosphate) and phosphate buffered saline (0.06 kΩ·cm, pH 7.2, Life Technologies, Ltd.); micropore dimensions of 7.5 μm height × 4.0 μm width × 80 μm length.

the measured signal amplitude data. Polystyrene particles (mean diameter of 3.10 μm) were used for these measurements. The height, width, and length of the micropore were 7.5, 4.0, and 80 μm, respectively. Increasing the applied voltage increases the signal amplitude value. When the applied voltage increases, the signal/noise (S/N) ratio can be enhanced. In conventional ionic current measurements, however, the background ionic current simultaneously increases with increasing the applied voltage.[22] Because of this limitation, most previous studies have utilized applied voltages ranging from only several hundred mV to several V. Therefore, the present method clearly differs from conventional methods in terms of the signal enhancement when increasing the applied voltage, and this highlights our method's superior characteristics. Our method had a S/N ratio of 240 for the applied voltage of 80 V (Figure 4a). Figure 4b shows the effect of the flow channel and bridge channel height (range from 5 to 60 μm) on the measured signal amplitude values. Smaller polystyrene particles (mean diameter of 1.00 μm) were used for these measurements. The height, width, and length of the micropore were 2.0, 2.0, and 14 μm, respectively. As can be seen in the figure, the signal amplitude values increased by increasing the height of the flow channel and bridge channel. Because the resistance of the micropore decreased as the channel height (volume) increased, the trend could be interpreted in terms of the increased ionic current for larger channels. Figure 4c shows the effect of electrolyte solution resistivity when varying TBE buffer concentration. A more resistive electrolyte solution suppressed the signal amplitude values due to the smaller ionic current. This trend was also found even for different buffer solutions (phosphate buffer and phosphate buffered saline), as shown in Figure 4d. These series of measurements highlight that the sensitivity of our method can be enhanced by an increase of ionic current through the higher applied voltage, the lower channel resistance and the lower resistivity of electrolyte solution without an increase of background current when using the microfluidic bridge circuit.

Finally, we carried out the detections of nanoparticles with the sensitivity of 0.01% of the pore volume and the detections of biorelated samples, as shown in Figure 5a, to demonstrate

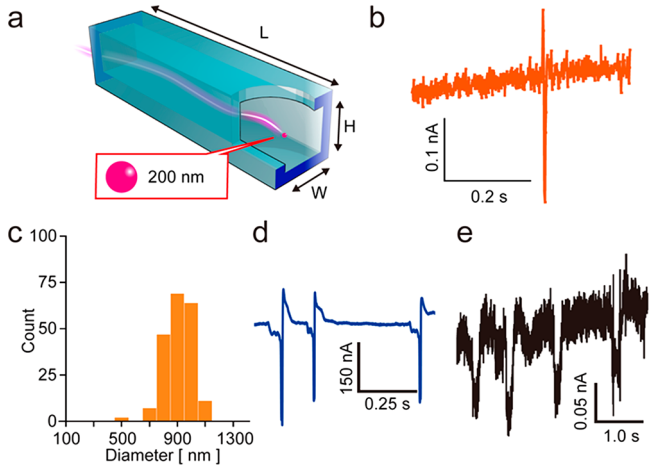

Figure 5. Detection of nanoparticles, bacteria, cancer cells, and DNA molecules in the microfluidic bridge circuit. (a, b) Schematic illustration and signal for detection of 200 nm diameter particles; micropore dimensions of 2.0 μm height × 2.0 μm width × 14 μm length. (c) Size distribution of *Staphylococcus epidermidis* obtained using our method; micropore dimensions of 7.0 μm height × 3.0 μm width × 8.0 μm length. 200 cells of the cultured *S. epidermidis* were introduced into the micropore and detected for 140 s. (d) Signals for HeLa cells in cell culture medium (0.006 kΩ·cm); micropore dimensions of 20 μm height × 10 μm width × 10 μm length. (e) Signals for T4 DNA molecules; micropore dimensions of 7.5 μm height × 4.0 μm width × 80 μm length.

the applicability of the microfluidic bridge circuit. Figure 5b shows the time series data of measured ionic current signals. Polystyrene nanoparticles (mean diameter of 200 nm) were used for these measurements. The height, width, and length of the micropore were 2.0, 2.0, and 14 μm, respectively. A clear peak signal was observed, as shown in Figure 5b. The obtained data demonstrate that the sensitivity of the particle volume detection is 0.01% of the pore volume, because 200 nm particles have a volume of 4 aL and the 14 μm long micropore has a volume of 5.6 × 10^4 aL. These results highlight the advantage of our method that its sensitivity is 100 times higher than that of existing ionic current sensing methods (sample detection with the sensitivity of 1% of the pore volume). The conventional sensing methods can detect 200 nm diameter particles using a pore of 400 aL volume (1.4 μm height × 1.4 μm width × 0.2 μm length).[2,4,5,14,24−27] The measured signal

DOI: 10.1021/jacs.7b06440
J. Am. Chem. Soc. 2017, 139, 14137−14142

amplitude value for small nanoparticles of 200 nm diameter is consistent with the theoretically estimated value (see the Supporting Information). Furthermore, our method also allowed detection of bacterial cells, cancer cells, and DNA molecules, as shown in Figure 5c–e. We confirmed that the size distribution of *Staphylococcus epidermidis* was consistent with that of literature data,[29] and cancer cells and DNA molecules were detected in a long micropore.

CONCLUSION

In conclusion, we demonstrated a rational methodology that can detect samples with the sensitivity of 0.01% of the pore volume by measuring a transient current generated by the potential differences in a microfluidic bridge circuit. Our method substantially suppresses the background ionic current from the μA level to the pA level, which essentially lowers the detectable particle volume limit even for relatively large pore structures. Indeed, utilizing a microscale long pore structure, we successfully detected various samples including polystyrene nanoparticles, bacteria, cancer cells, and DNA molecules. Although we have used different pore dimensions to show the proof-of-concept clearly in this paper, researchers could use the one designed system for the recognition of various analytes. Furthermore, our method will expand the applicability of ionic current sensing systems for various mixed biomolecule samples with a wide size range, which had been difficult to measure by existing pore technologies. Combination of conventional pore technologies with our method should enable researchers to detect various sized samples serially in a single size-sensing chip without sample clogging of the micropore.

METHODS

Construction of the Electrical Circuit Including the Sensing Chip and Bridge Circuit for Ionic Current Sensing. Using photolithography techniques, we fabricated microchannels on a PDMS plate (SILPOT 184 Dow Corning, Toray Co., Ltd.). The sensing chip was fabricated by bonding a cover glass and the PDMS plate with the microchannels. Dimensions of the microchannels were observed with a laser microscope after fabrication. Microchannels were filled with electrolyte solution that had an electrical conductivity allowing current flow by the applied voltage. To suppress high frequency noise from other instruments in the room, the electrical circuit was placed in a shield box (Shield Room Corporation). We applied the high voltage and sensed the current using silver electrodes (FTVS-408, Oyaide), which were connected to reservoirs for the sample flow channels and bridge channels. Current flowing through the bridge channels was monitored by an Ampere meter that consisted of an amplifier (low noise current amplifier DLPCA-200, FEMTO), a signal converter (NI USB-6259, National Instruments), and handmade software made by Lab view (National Instruments). Voltages were supplied by batteries (6LR61YXJ/1S, Panasonic). The standard applied voltage of this study was 53 V. The 1-kΩ resistor (E-Globaledge Corporation) and variable resistor (7270, BI Technologies) were ordinary commercial resistors.

Preparation of Polystyrene Particles. Polystyrene microspheres (Fluoresbrite, Polyscience) of 0.2, 0.75, 1.00, 1.10, 1.75, 2.08, and 3.10 μm diameters were used as samples for current sensing. Purchased sample solution was diluted using distilled water to 2.5×10^{-3} w/v%.

Preparation of Bacteria, Human Cell, and DNA Molecule Samples. *Staphylococcus epidermidis* (ATCC 14990) was used as bacteria sample. *S. epidermidis* was cultured in 2.5% LB medium (LB Broth (Miller), Sigma-Aldrich, Co.) while shaking at 37 °C and diluted using PB to 10^7 cells/mL. HeLa cells (a cervical carcinoma cell line) were used as the human cell sample. HeLa cells were cultured in Minimum Essential Medium Eagle (MEM, M4655, Sigma-Aldrich Co.) at 37 °C and diluted with PBS to 2.5×10^5 cells/mL. The T4 DNA molecules (T4GT7DNA, Nippon Gene) were used as the DNA molecule sample. The T4DNA molecule solution was diluted with TBE buffer to 5 ng/mL.

Electrolyte Solution. The 5×TBE buffer (0.45 M Tris, 0.45 M boric acid, 0.01 M EDTA) was used as the standard electrolyte solution in this study. We used 10×TBE (0.89 M Tris, 0.89 M boric acid, 0.02 M EDTA) buffer and 20×TBE buffer (1.78 M Tris, 1.78 M boric acid, 0.04 M EDTA) to change the ζ-potential of polystyrene nanoparticles and resistivity of microchannels.

Proposed Theoretical Equation. Considering the signal amplitude-related parameters, we proposed eq 1 (its derivation is given in the Supporting Information):

$$I_{\text{signal}} = \frac{\Delta R_x}{R_{b1} + R_{b2} + R_{1\text{-k}\Omega} + R_x} \times \frac{V_s}{R_{s1} + R_{s2} + R_x} \quad (1)$$

where I_{signal} is signal amplitude, ΔR_x is resistance change of the micropore by sample introduction, V_s is applied voltage, R_{b1} and R_{b2} are resistances of bridge channels, $R_{1\text{-k}\Omega}$ is resistance of the 1-kΩ resistor, R_{s1} and R_{s2} are resistances of sample flow channels, and R_x is resistance of the micropore.

ASSOCIATED CONTENT

Supporting Information

The Supporting Information is available free of charge on the ACS Publications website at DOI: 10.1021/jacs.7b06440.

Supplementary figures; derivation and validation of theoretical equation; validation of accuracy of 200 nm particle detection result (PDF)

AUTHOR INFORMATION

Corresponding Authors

*yasaki.hirotoshi@e.mbox.nagoya-u.ac.jp
*yasui@chembio.nagoya-u.ac.jp
*yanagida@cm.kyushu-u.ac.jp
*kawai@sanken.osaka-u.ac.jp
*babaymtt@apchem.nagoya-u.ac.jp

ORCID

Hirotoshi Yasaki: 0000-0001-6985-9073
Takao Yasui: 0000-0003-0333-3559
Takeshi Yanagida: 0000-0003-4837-5701

Notes

The authors declare no competing financial interest.

ACKNOWLEDGMENTS

This research was supported by Grant-in-Aid for JSPS Research Fellow 15J03490, PREST(JPMJPR151B, JPMJPR16F4), JST, the JSPS Grant-in-Aid for Young Scientists (A) 17H04803, the ImPACT Program of the Council for Science, Technology and Innovation (Cabinet Office, Government of Japan), the JSPS Grant-in-Aid for Scientific Research (A) 16H02091, and the Cabinet Office, Government of Japan and the JSPS through the Funding Program for World-Leading Innovative R&D on Science and Technology (FIRST Program)

REFERENCES

(1) DeBlois, R. W.; Wesley, R. *J. Virol.* **1977**, *23*, 227–233.
(2) Harms, Z. D.; Haywood, D. G.; Kneller, A. R.; Selzer, L.; Zlotnick, A.; Jacobson, S. C. *Anal. Chem.* **2015**, *87*, 699–705.
(3) Zhou, K.; Li, L.; Tan, Z.; Zlotnick, A.; Jacobson, S. C. *J. Am. Chem. Soc.* **2011**, *133*, 1618–21.
(4) Goyal, G.; Mulero, R.; Ali, J.; Darvish, A.; Kim, M. J. *Electrophoresis* **2015**, *36*, 1164–1171.
(5) Asghar, W.; Wan, Y.; Ilyas, A.; Bachoo, R.; Kim, Y. T.; Iqbal, S. M. *Lab Chip* **2012**, *12*, 2345–52.

DOI: 10.1021/jacs.7b06440
J. Am. Chem. Soc. 2017, 139, 14137–14142

(6) Carlsen, A. T.; Zahid, O. K.; Ruzicka, J. A.; Taylor, E. W.; Hall, A. R. *Nano Lett.* **2014**, *14*, 5488−92.
(7) Clarke, J.; Wu, H. C.; Jayasinghe, L.; Patel, A.; Reid, S.; Bayley, H. *Nat. Nanotechnol.* **2009**, *4*, 265−70.
(8) Keyser, U. F.; Koeleman, B. N.; van Dorp, S.; Krapf, D.; Smeets, R. M. M.; Lemay, S. G.; Dekker, N. H.; Dekker, C. *Nat. Phys.* **2006**, *2*, 473−477.
(9) Li, J.; Gershow, M.; Stein, D.; Brandin, E.; Golovchenko, J. A. *Nat. Mater.* **2003**, *2*, 611−5.
(10) Menard, L. D.; Mair, C. E.; Woodson, M. E.; Alarie, J. P.; Ramsey, J. M. *ACS Nano* **2012**, *6*, 9087−9094.
(11) Nivala, J.; Marks, D. B.; Akeson, M. *Nat. Biotechnol.* **2013**, *31*, 247−50.
(12) Plesa, C.; Ruitenberg, J. W.; Witteveen, M. J.; Dekker, C. *Nano Lett.* **2015**, *15*, 3153−8.
(13) Ayub, M.; Hardwick, S. W.; Luisi, B. F.; Bayley, H. *Nano Lett.* **2013**, *13*, 6144−50.
(14) Shasha, C.; Henley, R. Y.; Stoloff, D. H.; Rynearson, K. D.; Hermann, T.; Wanunu, M. *ACS Nano* **2014**, *8*, 6425−6430.
(15) Freedman, K. J.; Bastian, A. R.; Chaiken, I.; Kim, M. J. *Small* **2013**, *9*, 750−9.
(16) Japrung, D.; Dogan, J.; Freedman, K. J.; Nadzeyka, A.; Bauerdick, S.; Albrecht, T.; Kim, M. J.; Jemth, P.; Edel, J. B. *Anal. Chem.* **2013**, *85*, 2449−56.
(17) Larkin, J.; Henley, R. Y.; Muthukumar, M.; Rosenstein, J. K.; Wanunu, M. *Biophys. J.* **2014**, *106*, 696−704.
(18) Li, W.; Bell, N. A.; Hernández-Ainsa, S.; Thacker, V. V.; Thackray, A. M.; Bujdoso, R.; Keyser, U. F. *ACS Nano* **2013**, *7*, 4129−4134.
(19) Plesa, C.; Kowalczyk, S. W.; Zinsmeester, R.; Grosberg, A. Y.; Rabin, Y.; Dekker, C. *Nano Lett.* **2013**, *13*, 658−63.
(20) Rodriguez-Larrea, D.; Bayley, H. *Nat. Nanotechnol.* **2013**, *8*, 288−95.
(21) Rosen, C. B.; Rodriguez-Larrea, D.; Bayley, H. *Nat. Biotechnol.* **2014**, *32*, 179−81.
(22) Bayley, H.; Martin, C. R. *Chem. Rev.* **2000**, *100*, 2575−2594.
(23) Jagtiani, A. V.; Carletta, J.; Zhe, J. *J. Micromech. Microeng.* **2011**, *21*, 065004.
(24) Song, Y.; Li, M.; Pan, X.; Wang, Q.; Li, D. *Electrophoresis* **2015**, *36*, 398−404.
(25) Yukimoto, N.; Tsutsui, M.; He, Y.; Shintaku, H.; Tanaka, S.; Kawano, S.; Kawai, T.; Taniguchi, M. *Sci. Rep.* **2013**, *3*, 1855.
(26) Han, Y.; Wu, H.; Liu, F.; Cheng, G.; Zhe, J. *Anal. Chem.* **2014**, *86*, 9717−22.
(27) Guo, J.; Chen, L.; Ai, Y.; Cheng, Y.; Li, C. M.; Kang, Y.; Wang, Z. *Electrophoresis* **2015**, *36*, 737−743.
(28) Yokota, K.; Tsutsui, M.; Taniguchi, M. *RSC Adv.* **2014**, *4*, 15886−15899.
(29) Antoci, V.; Adams, C. S.; Parvizi, J.; Davidson, H. M.; Composto, R. J.; Freeman, T. A.; Wickstrom, E.; Ducheyne, P.; Jungkind, D.; Shapiro, I. M.; Hickok, N. J. *Biomaterials* **2008**, *29*, 4684−4690.

DOI: 10.1021/jacs.7b06440
J. Am. Chem. Soc. 2017, 139, 14137−14142